Accepted manuscript
Cite as: P.L. Carotenuto, A. Della Cioppa, A. Marcelli, G. Spagnuolo, An Evolutionary Approach to the Dynamical Reconfiguration of PhotoVoltaic Fields, Neurocomputing, 170 (2015), 393-405.
http://dx.doi.org/10.1016/j.neucom.2015.04.094

An Evolutionary Approach to the Dynamical Reconfiguration of PhotoVoltaic Fields

P. L. Carotenuto[a], A. Della Cioppa[a], A. Marcelli[a], G. Spagnuolo[a,*]

[a] *DIEM, University of Salerno*
Fisciano (SA), 84084, Italy

Abstract

The dynamical reconfiguration of photovoltaic panels is a useful approach for fighting the detrimental effects of mismatching on their power production. The practical implementation of the method has been recently optimized by means of efficient and reliable relays. However, two problems remain still open. The first is to determine the optimal electrical connection among the panels that ensures the maximum power produced at the actual irradiance conditions, while the latter is to constrain the computation time of such optimal configuration to fit the need of real time applications.

We present an evolutionary approach to the first problem. It is designed for allowing a straightforward porting to an embedded system and it is aimed at reconfiguring photovoltaic panels, thus not modules like some other approaches do in literature. Simulation results confirm the reliability and convergence capabilities of the proposed method and encourage further work for the adoption of the algorithm in real time applications. The problem of minimizing the computation time is also addressed.

Keywords: Photovoltaic systems, maximum power production, dynamical reconfiguration.

*Corresponding author
Email addresses: pcarotenuto@unisa.it (P. L. Carotenuto), adellacioppa@unisa.it (A. Della Cioppa), amarcelli@unisa.it (A. Marcelli), gspagnuolo@unisa.it (G. Spagnuolo)

1. Introduction

The efficiency of a PhotoVoltaic (PV) panel is actually about 15%, but in real applications this figure is even lower because of many reasons. One of the reasons, occurring especially in urban context is the mismatched operating conditions at which the panels forming a PV plant work [10]. As some panels are connected in series in order to reach a voltage level that fits with the input specifications of the commercial inverters, the presence of a partial shadowing affecting some cells or other inhomogeneity among the parameters of the cells, e.g., due to aging, failures or manufacturing tolerances, might cause a significant drop in the power production [24]. Producers usually install bypass diodes in the panels for mitigating the power loss in case of mismatching, but these diodes greatly change the voltage vs. current (V-I) characteristic of the PV array. When the diodes enter into conduction for compensating a current mismatching among the cells of the string, the voltage vs. power (V-P) characteristic of the array shows more than one Maximum Power Point (MPP).

To obtain the MPP, the inverter control system is usually equipped with a Maximum Power Point Tracking (MPPT) algorithm and many methods have been proposed in literature with the aim to find the MPP, including Fuzzy Logic and Neural Networks [23, 29]. Unfortunately, such approches lack in versatility in that PV panels operate in conditions that vary with time. As a consequence, methods like Neural Networks, have to be trained periodically to guarantee an optimal MPP tracking. Moreover, while such methods perform well under uniform irradiance conditions in which only a single MPP is present, partial shading conditions described above cannot be managed by the MPPT algorithm, so that a further power drop might occur [10]. The problem can be solved by a distributed MPPT architecture, but at the price of a power processing that is active also when mismatched conditions do not occur or of an increased plant cost [2, 20, 31, 32, 33].

Dynamical reconfiguration of the electrical connection among the modules reduces the detrimental effect of the mismatching among modules and also allows to implement monitoring, diagnosis and prognosis functions.

Very few are the systems available on the market that allow to dynamically change the series/parallel connection among the panels in order to maximize the power produced by the PV field, as the one described in [34]. In the very recent literature, instead, some methods and techniques have been proposed, this being the confirmation of the interest of the scientific commu-

nity into an approach that is very promising with respect to the existing ones (e.g. [19, 30]). Some recent patents have also appeared (e.g. [26]).

Some algorithms are based on the estimation of the irradiance at which the panels in the PV field work. Such methods are inaccurate, because they cannot take into account the real operating conditions of the panels and also the possibility that some of their sections work differently. Thus, such methods do not allow to implement an effective monitoring of the field. Other approaches assume that detailed measurements are periodically performed on each panel. This approach allows to determine more accurately the new configuration to be entered and to collect data on which a diagnostic method for determining the panels state of health can be devised [6]. The drawback is the need of acquiring the electrical data concerning the panels behavior periodically. Nevertheless, the power loss deriving from the above drawback can be greatly reduced by suitably optimizing the measurement process.

The method proposed in this paper aims at maintaining high efficiency of the PV system in any conditions, including partial shading. The reconfiguration procedure has a first step consisting in the acquisition of the V-I characteristic of each panel in the PV field by means of a suitably controlled dc/dc converter. Once such characteristics are available, an optimization procedure determines the new connection among the PV panels ensuring that the maximum power is extracted from the PV field. Finally, a processor controls a set of switches for settling the new electrical configuration of the PV panels. The whole procedure is repeated periodically.

The first step needs few milliseconds per panel, this time having a lower bound depending on the internal capacitance of the cells the panel is made of. The third step depends on the type of relays used, but it is not expensive in terms of time. Instead, the second step, devoted to the computation of the best configuration to enter, might be very time consuming because the number of possible connections among the panels is be very high. The price to pay for a long computation time is that the PV field remains in an electrical configuration that is not the best one for the actual operating conditions of the panels, e.g., for the actual shading pattern affecting the PV field. The computation of the new configuration would not be a prohibitive task for a personal computer, but on-field applications require low costs and, thus, the employment of embedded systems, e.g. micro-controller, digital signal processors or field programmable gate arrays.

We propose the use of an Evolutionary Algorithm (EA) for implementing the second step, i.e., to determine the best configuration of the panels

of the PV field. The algorithm has been studied and designed for requiring low amount of memory and computation resources, with a high convergence capability and repeatability, so that it can be implemented on an embedded system almost straightforwardly. The algorithm is validated through the use of V-I characteristics obtained by PV panels physical models. The performances of the algorithm are documented by using a number of different scenarios occurring in real conditions. redAnyway, the minimization of computation time is only addressed and it will be extensively treated in a forthcoming paper.

To the best of authors' knowledge, EAs have been mainly used either to solve the MPPT problem under partial shading conditions for different PV fields fixed topologies [28, 22, 8, 18] or to design under static conditions large photovoltaic systems as well as hybrid energy systems [13, 16], including a number of renewable and classical energy sources, like wind or diesel.

The motivation behind the use of EAs for dynamical reconfiguration of PV fields is that they perform well when the objective function is non-linear, as occurs to the output characteristic of PV fields when their modules work under mismatched conditions. The problem complexity increases since each energy source has its own operating constraints and no deterministic algorithm could be effectively used to find the optimal solution in practical computation times.

2. Dynamical Reconfiguration of PhotoVoltaic Panels

2.1. PV field topology

Before discussing the PV panels reconfiguration process, we have to introduce the PV field topology we refer to. To this aim, we assume that each PV panel is made of a number of cells connected in series. Such cells are divided into a number of groups, named *modules*, each one having a bypass diode connected in anti parallel for minimizing the mismatching effects. Although the panels are physically arranged into a matrix, as shown in Figure 1, the electrical connection among them can be of different types. Here, the electrical topology of the PV field is assumed to be of series-parallel type. In other words, some panels are series–connected, forming *strings*, in order to reach a voltage complying with the inverter input specifications. Then, the PV strings are parallel-connected in order to increase the generated current and meet the inverter specifications in terms of power. As a consequence, a series-parallel topology composed by N_p panels organized into N_s electrically

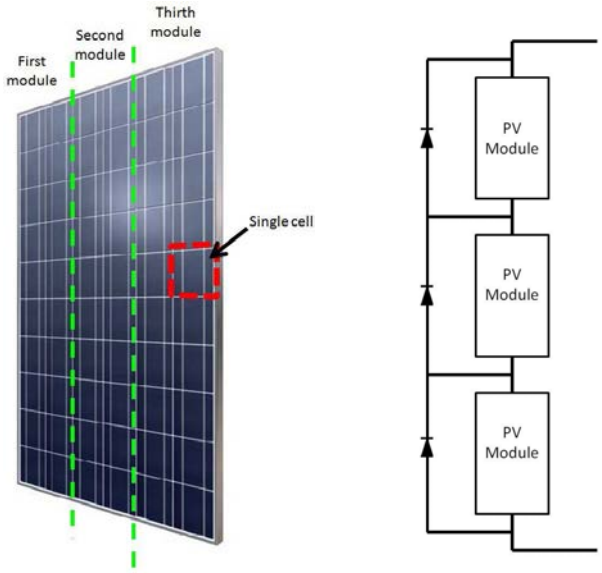

(a) Panel. (b) Electrical scheme.

Figure 1: PV panel: 1(a) reference model and 1(b) its electrical scheme.

parallel connected strings is considered. Thus, a PV panel belongs to one and only one string or, under particular irradiation conditions, it is disconnected from the PV field. According to the above topology, each arrangement of the panels into the strings represents a configuration of the PV field.

2.2. Photovoltaic panels reconfiguration process

The reconfiguration process adopted takes place periodically during the day and consists of three phases as follows:

1. in the first phase a suitably controlled dc/dc converter allows the acquisition of the V-I characteristic of each panel in the PV field. In particular, to the aim of computing the new electrical configuration to be settled in order to let the PV field produce the maximum power, it is assumed that a shading pattern for each PV panel is given. The shape of the shadow is defined and, by means of a simple and intuitive geometrical algorithm, the irradiance condition for each PV cell of each panel is calculated.
   In order to assign a unique irradiance value to each cell, the following assumptions have been done.

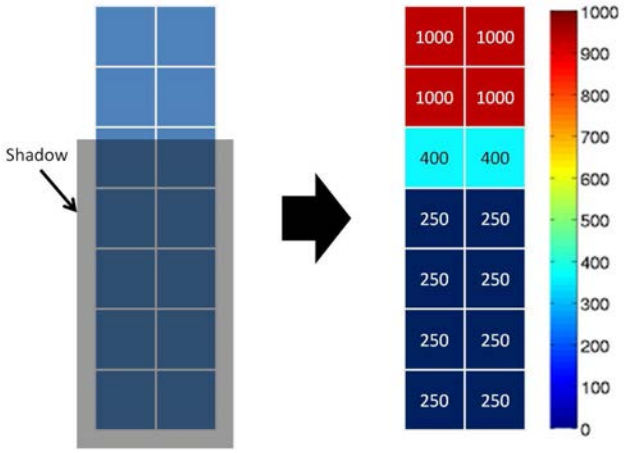

Figure 2: Example of shading pattern. In this example, there are three groups of cells: non-shaded cells, fully shaded cells and partially shaded cells. The first group is subjected to $G_{max} = 1000W/m^2$. The coefficient SO has been fixed at 0.75, so that the fully shadowed cells work at $G = (1 - 0.75 \cdot 1.0) \cdot 1000 = 250W/m^2$. The two partially shadowed cells work at an irradiance level equal to $G = (1 - 0.75 \cdot 0.8) \cdot 1000 = 400W/m^2$.

The solar irradiance of partially shaded cells G_{cell} has been related to the irradiance received by the non-shadowed cells, to the shading percentage and to the shadow opacity, as follows:

$$G_{\text{cell}} = (1 - SO \cdot SP) \cdot G_{\text{max}} \tag{1}$$

where G_{max} is the irradiance received by no-shadowed cells, SP is defined as the percentage of the cell area subjected to shading and SO is defined so that $SO = 1$ when the irradiance is zero and $SO = 0$ when the irradiance is equal to G_{max}. Figure 2 shows an example of shading pattern for a number of cells.

Once the cell irradiance values are evaluated, the V-I characteristic of each panel is computed by applying, for each cell, the single-diode model including the Bishop contribution [5, 21].

After that the V-I characteristic of each PV panel is computed, it is possible to compute the same characteristic for the whole field, if a PV field series-parallel electrical structure is assigned, as discussed in the previous subsection.

2. In the second phase, an optimisation procedure looks for the best connection among the PV panels by computing the resulting electrical

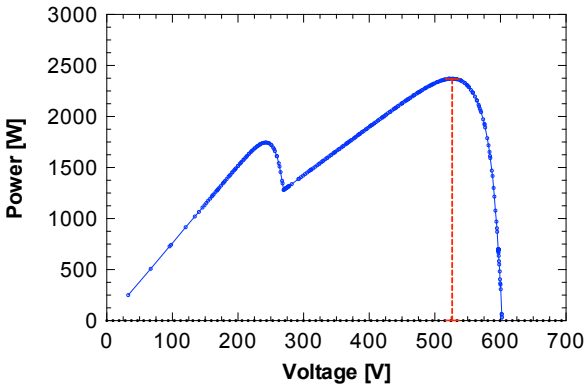

Figure 3: The absolute maximum of V-P characteristic (red circle).

power of the proposed solutions on the basis of the V-I characteristics previously obtained. The electrical power is determined under the given solar irradiance conditions by analyzing the acquired V-I characteristics of each panel and ensuring that the maximum power is extracted from the PV field.

The computation is executed through the following steps:

(a) once all panels characteristics have been acquired, the V-I characteristic of each string is obtained by doing a current sweep over a fixed number s of samples of the characteristics of all the panels belonging to that string;

(b) a voltage sweep is operated on the string V-I characteristics in order to obtain the V-I characteristic of the whole PV field;

(c) finally, the absolute maximum of the PV field V-P characteristic is computed:

$$P_{\max} = \max\{P_0, \ldots, P_i, \ldots, P_{s-1}\} \tag{2}$$

where $P_i = V_i \cdot I_i$ is the power of the i–th sample of the PV plant characteristics. An example of V-P characteristic and its maximum is reported in Figure 3.

3. Finally, in the last phase, a processor controls a set of switches for settling the new electrical configuration of the PV panels.

It should be noted here that, in real conditions, the reconfiguration process takes place every 30-40 minutes. However, although the optimization

of this time interval represents a challenging task deserving further research activity [7], it is out the scope of this paper. As a consequence, our aim is to achieve the optimal solution in the shortest time.

In the following section, the proposed evolutionary approach for searching the best configuration of the PV field is introduced and discussed with particular emphasis to the main implementation aspects related to the problem at hand.

3. Evolutionary approach to photovoltaic panels reconfiguration

Evolutionary Algorithms [4, 3] are based upon neo-Darwinian principles of evolution. They are population-based metaheuristic optimization approaches to problem-solving where multiple candidate solutions are maintained in parallel. Genetic search mechanisms are applied to breed high-quality solutions as subsequent generations are created using fitness-based selection. The fitness of a candidate solution is related to the objective function of the problem at hand and represents a measure of its quality at solving that problem.

The advantage of EAs compared to other optimization methods is that they makes only few assumptions about the underlying objective functions. Furthermore, the definition of objective functions usually requires only few information about the structure of the problem space. Finally, they are able to provide a good solution in a reasonable time. As a consequence, EAs perform consistently well in many different problem domains.

All Evolutionary Algorithms proceed in principle according to the following scheme:

1. initially, a fixed-size population of individuals with a random genome (the encoding that is adopted by each member of the population to solve a specific problem type) is created;
2. the values of the objective function are computed for each solution candidate in the current population. Depending on the problem at hand, this evaluation may incorporate complicated simulations and computations;
3. with the objective function, the utility of the different features of the solution candidates have been determined and a fitness value can now be assigned to each of them;
4. a subsequent selection process filters out the solution candidates with bad fitness and allows those with good fitness to enter the mating pool

with a higher probability. Without loss of generality, if the fitness is subject to maximization, the higher the fitness values are, the higher is the (relative) utility of the individuals to whom they belong;

5. in the reproduction phase, offspring is created by varying or combining the genotypes of the selected individuals by means of genetic operators. These offspring are then subsequently integrated into the population;
6. finally, if a termination criterion is met, the evolution stops, otherwise, the algorithm continues at step 2.

Among all the EAs, Genetic algorithms (GAs) [12] are well suited for facing the optimal arrangement of the panels among the photovoltaic strings, in that GAs are a subclass of EAs where the elements of the search space (genotypes) are binary strings or arrays of other elementary types. The genotypes are used in the reproduction operations, whereas the values of the objective functions are computed on basis of the phenotypes in the problem space which are obtained via a genotype-phenotype mapping.

In the context of dynamic reconfiguration of the PV field, the crucial tasks are the choice of the encoding [25], of the fitness function and of the genetic parameters to be used.

3.1. Encoding

The simplest representation of the individual is an array of N_p integers $\mathbf{g} = [g_1, \cdots, g_i, \cdots, g_{N_p}]$. The generic integer g_i belongs to the interval $A = [0, N_s]$, where N_s is equal to the number of PV strings under consideration and the value 0 means that the panel does not belong to any string, i.e., it is disconnected from the PV field. In fact, since each panel can be connected to only one string or be disconnected from the PV field, each symbol value can be set as follows:

$$g_i = \begin{cases} j \in [1, \cdots, N_s] & \text{if the } i\text{–th panel is connected to the } j\text{–th string} \\ 0, & \text{if the } i\text{–th panel is disconnected} \end{cases}$$

Since any possible combination of integers belonging to the set A is valid, the total number of solutions is equal to $(1 + N_s)^{N_p}$.

3.2. Fitness Function

In order to compute the fitness of a solution, the proposed GA firstly maps a genotype $\mathbf{g}$ to the corresponding electrical configuration of the panels, then

it computes the resulting electrical power under given solar irradiance conditions by analyzing the acquired V-I characteristics of each panel as described in the subsection 2.2. In other words, we adopt as fitness function the maximum electrical power as computed by the eq. (2). In order to obtain feasible values for the fitness, a minimum voltage boundary is required to power on the inverter. On the other hand, the highest voltage boundary depends on safety standards. As a consequence, any electrical configuration for which inverter voltage constraints aren't respected is discarded by assigning to it a fitness value equal to zero. Thus, the fitness function becomes:

$$\Phi(\mathbf{g}) = \begin{cases} P_{\max} & \text{if } V_{\text{Inv}} \in [V_{\text{Inv}}^{\min}, V_{\text{Inv}}^{\max}] \\ 0 & \text{otherwise} \end{cases} \tag{3}$$

3.3. Genetic Parameters

As regards the selection scheme and the genetic operators to be used we have chosen the tournament selection, the uniform recombination and the bit–flip mutation.

Tournament selection is one of the most popular and effective selection schemes. According to it, T_s (tournament size) elements are picked from the population and compared with each other in a tournament. The winner of this competition will then enter mating pool. Although being a simple selection strategy, it is very powerful and therefore used in many practical applications. In fact, tournament selection leads to a lower *selection pressure* over population individuals. By this way, couples of individuals having very different chromosomes are more likely to be chosen for recombination.

Once a couple of individuals $(\mathbf{g}_i, \mathbf{g}_j)$ is selected, uniform recombination generates an offsring $\mathbf{o}$ as follows:

$$o_k = \begin{cases} g_k^i, \text{with probability } p_r \\ g_k^j, \text{with probability } (1-p_r) \end{cases} \qquad k \in [1, \cdots, N_s]$$

Finally, a bit–flip mutation operator is applied to the offspring by simply flipping integers in the genotype $\mathbf{o}$ with a probability p_m.

3.4. Problem complexity

According to both the enconding and the fitness function chosen, it should be noted that among all configurations, only a few number could be considered as good candidates for being the optimal one, since they achieve a high

power and, at the same time, they respect the inverter voltage boundaries discussed above. Given a fixed number of panels, the chosen representation leads to increase the space of solutions with the number of strings considered. Anyway, different solutions having the same maximum generated power value might be obtained. These solutions can be defined as 'equivalent'. In particular, two different classes of equivalence exist:

1. in the first class of equivalence, a solution is equivalent to another one if all the panels belonging to a couple of strings are mutually swapped;
2. in the second class of equivalence, solutions are equivalent if couples of panels assigned to different strings have the same V-I characteristic and are swapped among the strings they belong to.

While the number of equivalent solutions belonging to the first class depends only on the number of strings, the number of equivalent solutions belonging to the second class depends on the actual shape of V-I characteristics of PV panels and it cannot be estimated *a priori*. For this reason, the quantity:

$$\frac{(1+N_s)^{N_p}}{N_s}$$

represents an upper bound for the number of unique solutions, once the number of panels and strings have been assigned.

It should be stressed that this redundancy, while seems to be advantageous, can lead to a serious drawback in getting the optimal solution. In fact, the problem gets an additional twist if it is considered that, given a solution, either deactivating one panel or assigning it to a different string can deeply influence the behaviour of other panels (epistasis [9]) and, consequently, can lead to a rugged fitness landscape, i.e., unsteady or fluctuating (ruggedness [15]).

In biology, epistasis [9] is defined as a form of interaction between different genes, while in optimization, it is the dependency of the contribution of one gene (to the value of the objective function) on the state of other genes. Obviously, a problem is maximally epistatic when no proper subset of genes is independent of any other gene. Epistasis is mainly an aspect of the way in which the genome and the genotype-phenotype mapping are defined and has a strong influence on the search effectiveness. If one gene can turn off or affect the expression of other genes, a modification of this gene will lead to a large change in the features of the phenotype. Hence, the causality will be weakened and ruggedness ensues in the fitness landscape. As a consequence,

it becomes complex to define search operations with both good explorative and exploitive characters. In fact, optimization algorithms generally depend on some form of gradient in the fitness function. The landscape should be continuous and exhibit low total variation, so the optimizer can descend the gradient easily. When fitness functions are rugged, as in the case under study, it becomes complex for the optimization process to find the right directions to proceed to. The more rugged a function gets, the harder it becomes to optimize it.

Hence, although the problem of the rearrangement of photovoltaic panels seems at a first glance straightforward, from the above considerations it follows that it is very challenging in that we deals with both an epistatic genome and a rugged landscape.

4. Simulations

The proposed GA, developed in ANSI C language, has been tested on the 4 different solar irradiance scenarios realized by means of a simulator. After a preliminary tuning phase, throughout all the simulations execution the parameters have been set as summarized in Table 1. To better evaluate the effectiveness and the efficiency of the proposed method in facing the problem at hand, it is important to compare its results against those achieved by a top performing algorithm as the Random Mutation Hill Climber (RMHC) [11, 17]. In RMHC, a solution is chosen at random and its fitness is evaluated. The solution is then mutated at a randomly chosen single locus, and the new fitness is evaluated. If the mutation leads to an equal or higher fitness, the new solution replaces the old string. This procedure is iterated until the optimum has been found or a maximum number of function evaluations has been performed. This simple algorithm significantly outperforms GAs on many difficult problems as it is reported in [11, 17]. Aiming at carrying out this comparison, the RMHC has been implemented and run on the same scenarios allowing the same number of evaluations as for the GA. All the simulations for both the algorithms have been carried out on an Apple iMac equipped with 16 GB of memory and Intel i7 Quad-core CPU running at 3.4 GHz.

4.1. Simulation framework

To investigate the effectiveness of the proposed approach, Axitec AC-250M/156-60S panel [1] has been considered for the simulations. The panel

Table 1: Genetic Algorithm simulation parameters.

Population size	100
Number of generations	200
Tournament size	10%
Mutation rate	0.042
Recombination rate	0.9
Number of runs	20

Table 2: Photovoltaic cell parameters calculated from Axitec AC-250M/156-60S panel characteristics [1].

N_p	N_s	J_{sat}	R_s	n	R_{sh}	V_{br}	m	a
24	2	1.26 nA	1 mΩ	1.5	1 kΩ	-15 V	3	0.002

is $991mm \times 1665mm$ sized and it has three series-connected modules, each one protected by a bypass diode, as shown in Figure 1(b). All modules have 20 cells in series organized into two vertical lines of 10 cells, so that the panel is a 10×6 matrix of PV cells. The parameters of the PV plant, of the solar cells and of the Bishop model used in the simulations are listed in Table 2.

A simulator has been used for defining graphically the shadowing pattern affecting the 24 panels, physically organized in two rows, and for obtaining the V-I characteristics of the panels themselves. As in practical applications, a reasonable number of (I,V) samples for each PV panel curve has been set equal to 100. Moreover, the operating constraints for the inverter voltage to be used in the fitness function (3) are $V_{\text{Inv}}^{\min} = 200V$ and $V_{\text{Inv}}^{\max} = 700V$.

Five different cases, each one corresponding to a different scenario, have been taken into account by considering the most likely shading causes, such as buildings, poles and cables, clouds, birds dropping, frost or dust.

In all scenarios, SO appearing in (1) has been fixed to 0.75, while SP depends on the percentage the cell area shaded. Finally, for each case, the following plots have been produced: i) solar irradiance chart of all cells of PV plant. Here, all panels have been separated by a bold vertical segment. The cells are represented as a grid; ii) V-I characteristics of each panel. These characteristics have been produced by using the method in [21], with the parameters values summarized in Table 2.

4.1.1. Shadows having a sharp shape: case 1

Buildings or the same PV panels could generate shadows having a sharp shape on some panels. Here, partial shading of one of the two PV panels is considered. In this case, quite all partially shaded panels have a strongly reduced current since the sharp shadow cover all their modules. In particular, only one partially shaded panel has only one shaded module. For this reason, there are six panels that generate a low current at any voltage value. Instead, the unique panel having only one shaded module works at a voltage that strongly depends on the current. The solar irradiance chart is shown in Figure 4(a) (left), while the V-I characteristics in Figure 4(a) (right).

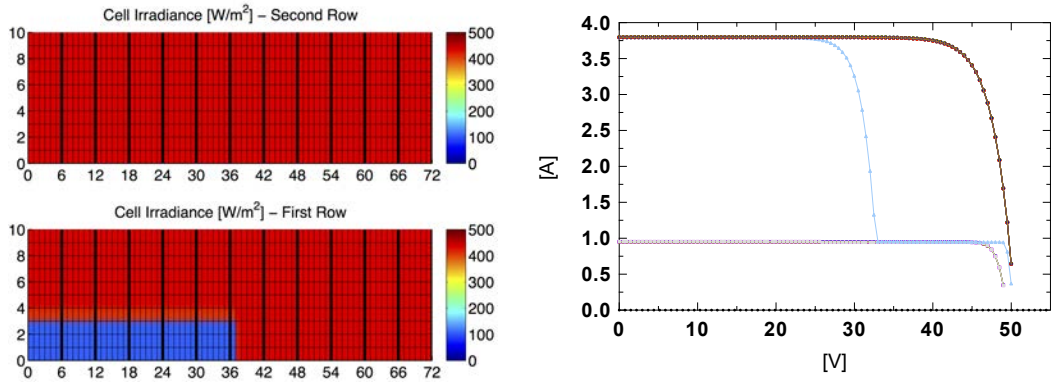

(a) Sharp shadowing. Solar Irradiance and voltage-current characteristics of PV panels. Shadow affects partially 7 panels of a row, strongly reducing solar irradiance.

Figure 4: Shadows having a sharp shape. Top pane: first case. Bottom pane: second case.

4.1.2. Diagonal shadowing: cases 2 and 3

The presence of light poles or cables generates, during some hours of the day, undesirable shadows which reduce the amount of the generated PV power. Also in this case, two different cases have been considered: shadow of a pole and shadow due to a cable. In the first one, a 3-4 cells wide shadow diagonally covers the simulated PV field, as shown in Figure 5(a). Even if this shadow could not be very wide, it covers all modules of partially shaded panels. For this reason, all these panels generate a very low current independently of their voltage. The V-I characteristics can be divided in three groups, with a high and with a low short circuit current having one MPP and with more than one MPP, respectively. This is shown in Figure 5(a) right.

Another case is the shadow of a cable or any linear thin obstacle covering a PV field. The main difference with respect to the previous scenario is the lack of a sharp shading. In Figure 5(b) (left), the shaded cells have very different solar irradiance values, due to the absence of fully shaded cells. In fact, no cell has an irradiance equal to minimum value, since the shadow is always thinner than the cell width.

In this case, only two of six partially shaded panels, due to the vertical orientation of modules, lead to a V-I characteristic having a unique current level. Instead, the voltage-current curves of the other shaded panels have two or three different current levels (see Figure 5(b) right).

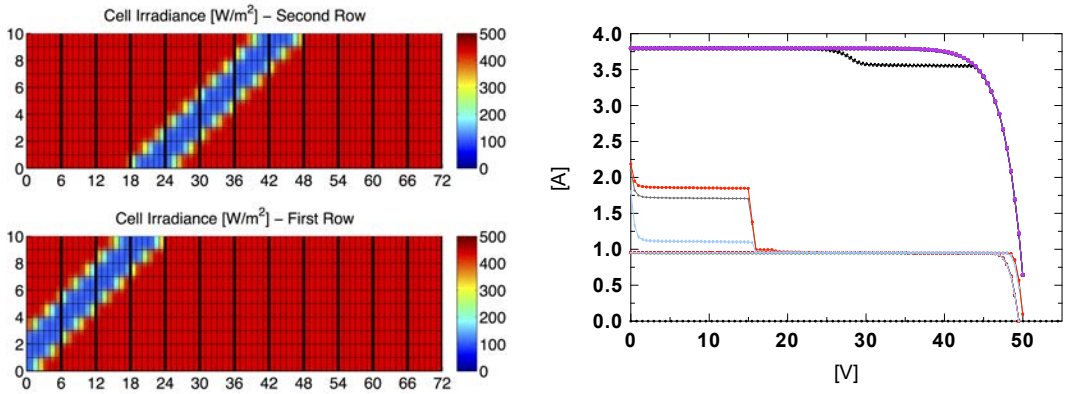

(a) Shadow of a pole. Solar Irradiance and voltage-current characteristics of PV panels.

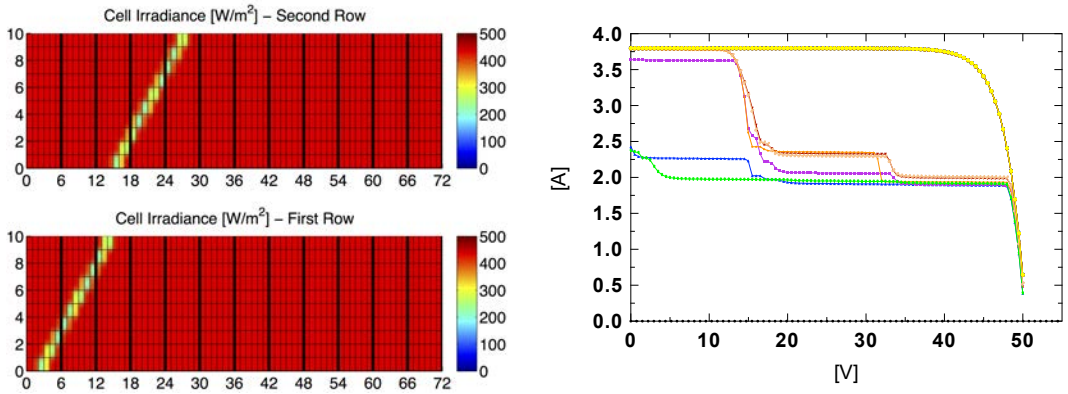

(b) Shadow of a cable. Solar Irradiance and voltage-current characteristics of PV panels.

Figure 5: Diagonal shadowing. Many panels, even if only partially shaded, cannot generate an high current due to the vertical orientation of their modules. Top pane: third case. Bottom pane: fouth case.

4.1.3. Gradual shadowing: case 4

This scenario can occur in presence of transient clouds having a heterogeneous density or when the panels are mounted on bended surfaces.

When dealing with an asymmetrical gradual shadow, the effects of both different levels of solar irradiance and a heterogeneous density obstacle (such as a tree or a cloud) have been considered. In Figure 4.1.3 (left), in both panels rows, all left-sided panels have been affected by a homogeneous shadow, similarly to the second scenario discussed above. Moreover, an heterogeneous shadow has been added to the second panels row (blue colored cells). All the panels interested by an heterogeneous solar radiation exhibit more than one MPP (see Fig. 4.1.3).

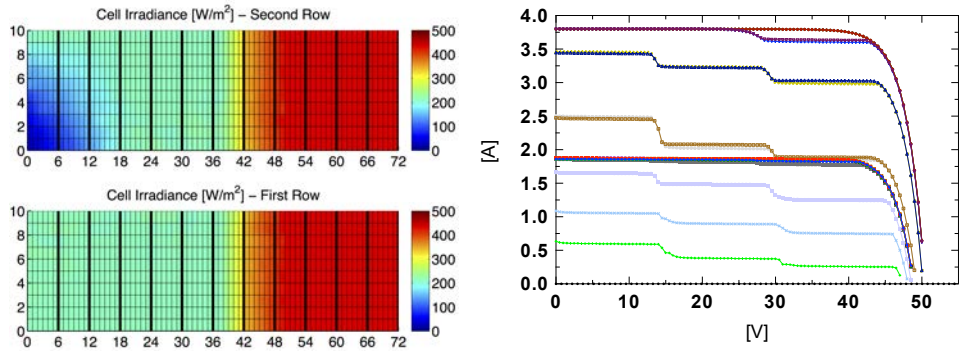

Figure 6: Asymmetrical Gradual Solar Irradiance. Solar Irradiance and voltage-current characteristics of PV panels. The left-sided panels of the two rows receive a different amount of solar energy.

4.1.4. Spot shadowing: case 5

As final case, the effects of dust, frost or birds dropping on PV panels has been analyzed. If an obstacle covers a cell, the current generated by the module containing that cell is inexorably reduced. For this reason, the size of shadow affects the V-I characteristics of each photo-voltaic panel.

The solar irradiance chart in Figure 7 (left) exhibits many shadow spots of different opacity and size. Generally, these kinds of shadows happen very often, especially when the cleaning of panels is not performed on a regular basis. Even if the percentage of shading of each panel is low, a considerable mismatching of PV panel characteristics has been verified (see Fig. 7 right).

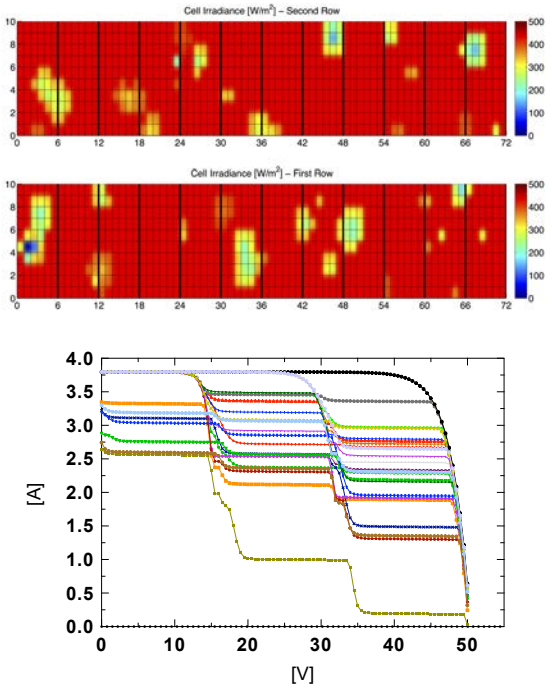

Figure 7: Spot shadowing: case 5.

4.2. Results

First of all, the best configurations chosen by GA are compared with to the default configuration, i.e., the static configuration in which all the panels are connected and arranged according to two separated strings. In Table 4.2 the power values obtained by the default and the best configurations chosen by GA are reported. The cases under examination have been sorted by increasing complexity of the reconfiguration problem and by fixing the shadow strength to 75%. As it is evident, the best configuration chosen by GA increases the power generation in all cases, especially when the two panels rows work under asymmetric conditions or the shadow doesn't exhibit a well-defined geometrical scheme, as it occurs for gradual or random solar radiance scenarios.

It is worth noting that a prediction of the power gain/loss ensured by the reconfiguration process is complex to be given. Indeed, it depends on the sequence adopted for disconnecting the panels from the strings in order to measure their V-I curve, to the frequency of the reconfiguration process, to the time needed for setting up the new calculated configuration, to the

type and permanence of the shadow, on the actual irradiance level (shiny or cloudy day). For instance, as for the procedure adopted for measuring the panels V-I curves, it is reasonable to assume that one panel at a time is disconnected, its V-I curve measured, and the same panel reconnected for doing the same with another panel. The worst case, assuming that all the panels are disconnected at the same time, is very unpractical because of the problems it should give to the inverter behavior. Indeed, in this case, the risk is that the inverter switches off because of the null power sensed at its input for a long time interval. As a consequence, in practical cases, the energy loss due to the reconfiguration process is negligible with respect to the energy gain ensured by the entering of the optimal configuration.

Case	**Power [W] (default)**	**Power [W] (GA)**	**Variation**	**CPU Time**
Sharp shadowing	2372.24	2748.52	+15.86%	$\backsim 7s$
Pole shadowing	2187.76	2258.59	+3.24%	$\backsim 71s$
Cable shadowing	2993.32	3007.69	+0.48%	$\backsim 61s$
Asymmetric gradual shadowing	1510.00	2199.98	+45.69%	$\backsim 267s$
Spot shadowing	2194.03	2362.02	+7.66%	$\backsim 296s$
		2365.44	+7.81%	
		2407.85	+9.74%	

Table 3: Comparison among power values of default and best configurations.

For each algorithm and for each problem Table 4 reports the best final value Φ_b, achieved after 20 runs with different random number generator initializations, the average value $\langle \Phi_b \rangle$ over the 20 final values, and the related standard deviation σ_Φ. With reference to such indexes, the table shows in bold the algorithm with the best value for each problem. As a first remark, the superiority of the GA with respect to RMHC in terms of performance is evident. In fact, the proposed GA outperforms RMHC in terms of all the indexes. The reason behind the poor performance of the RMHC is that once a good solution has been found, the time to discover a better one can be very longer, since many of the function evaluations are wasted on testing deleterious mutations of the actual solution due to the ruggedness of the fitness landscape. In other words, the probability of being trapped in a local optimum becomes very high. This problem does not take place for the GA for several reasons. First of all, GAs are implicit parallel [14], i.e., each individual

	GA			RMHC		
Case	Φ_b	$\langle\Phi_b\rangle$	σ_Φ	Φ_b	$\langle\Phi_b\rangle$	σ_Φ
1	**2333.70**	**2333.70**	**0**	2308.71	2300.72	5.40
2	**2258.59**	**2258.59**	**0**	2253.66	2241.51	9.76
3	**3007.69**	**3007.69**	**0**	2992.53	2924.92	58.08
4	**2212.06**	**2196.41**	**31.74**	1888.21	1845.05	52.18
5	**2407.85**	**2397.08**	**19.16**	2241.99	2186.72	41.27

Table 4: Experimental findings.

in the population is an instance of many different schemas of solution, and if the population is large enough, a large number of such different schemata are being sampled in parallel. Secondly, selection should conserve instances of such schemas during the evolution. Finally, a high crossover rate should quickly combine good blocks on different genotypes to create new solutions with higher fitness. The behaviour just described is more evident as the landscape ruggedness increases, as in the cases 3, 4 and 5. In fact, when the number of V-I characteristics evidenced by the PV field is higher (see Figure 6 and 7), the landscape ruggedness increases too and the differences between the performance of the two algorithms become larger.

Nevertheless, a statistical analysis to assess which algorithm is the best one in terms of average fitness has been performed: the results are reported in the next subsection.

The CPU time required to execute a single run of the GA depends on the case faced and ranges from a minimum of about 10 seconds in the best case to a maximum of about 300 seconds in the worst case. Anyway, except for the spot shadowing scenario, in all the cases under examination the GA is able to provide the best solution in about 20 generations, which means a CPU time of few seconds. RMHC shows very similar CPU times, the differences being related to the different genetic mechanisms between the algorithms. Even if GA performances are really appreciable, the time required to compute a fitness value, i.e., the most time-consuming part of the algorithm, is actually significant. In fact, the amount of time needed for this computation strongly depends on the number of samples we use for sampling the voltage-current characteristics of PV panels. So, in the worst case a run can last even many minutes, before evolution can found a suitable solution. This time is too long to quickly react to temporary shading phenomenons. Moreover, during this very long time interval, even if a shadow persists on PV plant, the

environmental conditions could be changed. So, after this time, the solution found could be not suitable for the new conditions.

Yet, execution time must be further reduced, to the aim of porting the GA on an embedded system, by improving the fitness computation time. To this end, we have performed pilot experiments with the aim to reduce the number of samples in V-I characteristics of panels by means of an optimized point decimation method following [6]. Preliminary results show that in the worst case (case 6) a single GA run takes about 7 seconds. This means that on an embedded system like a Beagle Board XM the required time for each GA execution is close to 1 minute.

4.2.1. Statistical analysis

To compare the GA and the RMHC from a statistical point of view, a classical approach based on nonparametric statistical tests has been carried out, following [27]. in particular, the Wilcoxon Signed Rank test is a non-parametric test used to determine whether two matched groups of data are different. The Wilcoxon Signed Rank test is robust in that it does not require the data to have a Gaussian distribution. As is common with hypothesis testing in general, it has been start out with a Null Hypothesis, which can be thought of as our default assumption. The Null Hypothesis for the Wilcoxon Signed Rank test is that the two groups of data are not different. Based on the W statistic, which is calculated from the data, it is determined whether to accept or reject the Null Hypothesis. In presence of a large enough number of samples (over 25), it is possible to use the calculated p-value to either accept or reject the Null Hypothesis. For a smaller sample size, it is read off the critical value of W from a table, and if the calculated W statistic is below the critical W value the Null Hypothesis is rejected. The p-value is the probability of obtaining either the observed difference or a more extreme value of the difference between the two groups, purely based on chance. If the p-value is below a threshold value, the Null Hypothesis is rejected and the result is considered significant. On the other hand, if the p-value is greater than the threshold value, the Null Hypothesis is accepted.

The statistic for Wilconxon p-value is 28.0 with 1 and 5 degrees of freedom. The p-value for Wilconxon is 0.015625. The W–value is 0, while the critical value of W for 7 at $p \leq 0.05$ is 2. Therefore, the result is significant at $p \leq 0.05$, i.e., the Null Hypothesis is rejected. In other words, the statistical analysis confirms that the proposed GA outperforms the RMHC.

4.3. Case analysis

In order to discuss in detail the simulation results, for each scenario, we report the graphical synopsis of the optimal solution, where the panels assume a different color according to the string they belong to (red means string 1, green string 2 and white means that a panel is disconnected), the V-P characteristic of the optimal solution and, finally, the evolution of the best fitness for each generation averaged over all the 20 runs and its standard deviation. It should be evidenced here that we discuss only the results provided by the GA because those provided by RMHC never get better configurations.

4.3.1. Shadows having a sharp shape

Case 1 (see Fig. 4(a)). The GA produces, at the end of all the 20 runs, always the same electrical configuration. A graphical representation of this solution is shown in Figure 8(a). It is evident that the best configuration is obtained by disconnecting all the shadowed panels. The remaining panels are arranged into two identical strings. Since all the panels forming the optimal solution have exactly the same V-I characteristic, there are many equivalent ways to arrange them in the two PV strings having the same identical V-P characteristic.

The V-P characteristic of the optimal configuration shows only one MPP, as shown in the Figure 8(b), corresponding to a power equal to 2748.53W @ V_{mpp} 380.81V, while the MPP value is equal to 2372.24W @ V_{mpp} 528V for the default configuration.

This solution is obtained in a very few amount of generations, as shown in Figure 8(c), where for each generation the best fitness (MPP) value averaged over the 20 runs (blue solid line) and its standard deviation (red dotted line) are plotted.

The highest maximum power is obtained at the end of all the twenty runs in less than 20 generations. In fact, after the 20th generation, the standard deviation collapses to zero.

4.3.2. Diagonal shadowing

Case 2. (see Fig. 5(a)). The proposed GA disconnects all the partially shaded panels as occurs in previous scenario.

The remaining panels are re-distributed among the two photovoltaic strings (see Figure 9(a)). The decision taken by the GA leads to a V-P characteristic having one MPP corresponding to 2258.59W @ V_{mpp} 312.00V, while the

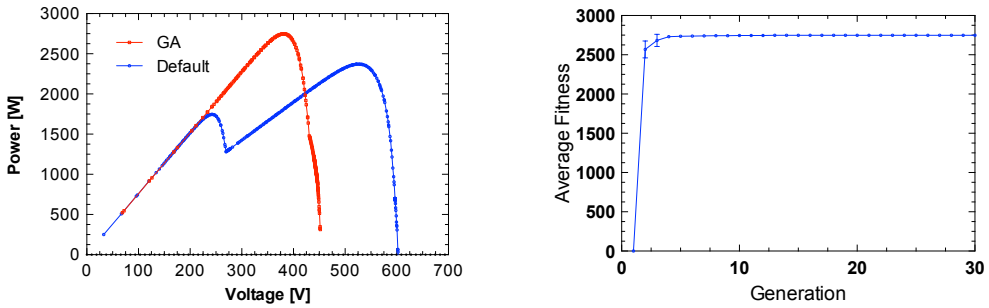

(a) (b)

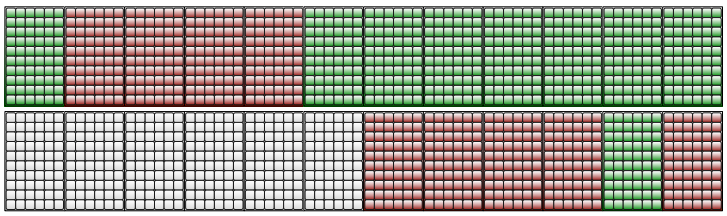

(c)

Figure 8: Partial shading of one of the two PV panels rows. Top pane (a): Voltage-Power characteristics of the PV field. Best solution obtained by the GA (blue line), default configuration (black line). Top pane (b): evolution of the best fitnesses averaged over 20 runs. Mean fitness (blue line) +/− standard deviation (red dotted line). Bottom pane (c): electrical configuration chosen by the GA.

standard configuration shows a MPP equal to 2187.76W @ 305.1V, as shown in Figure 9(b).

As in previous scenarios, the fitness trend is very abrupt (see Figure 9(c)), i.e. the optimal solution has been found in less than 20 generations, or equivalently in less then 2000 evaluations of the fitness function.

Case 3. (see Fig. 5(b)). In this case, due to the vertical orientation of modules, only two of six partially shaded panels have only one current level in their V-I characteristics. Instead, the V-I characteristics of the remaining shaded panels have two or three different current levels (see Figure 10(b)).

In the best configuration, the solution proposed by the GA disconnects only the panels having all modules covered by the cable shadow.

As in the previous scenario, in order to obtain a symmetrical solar irradiance pattern on two rows, the panels are arranged as shown in Figure 10(a).

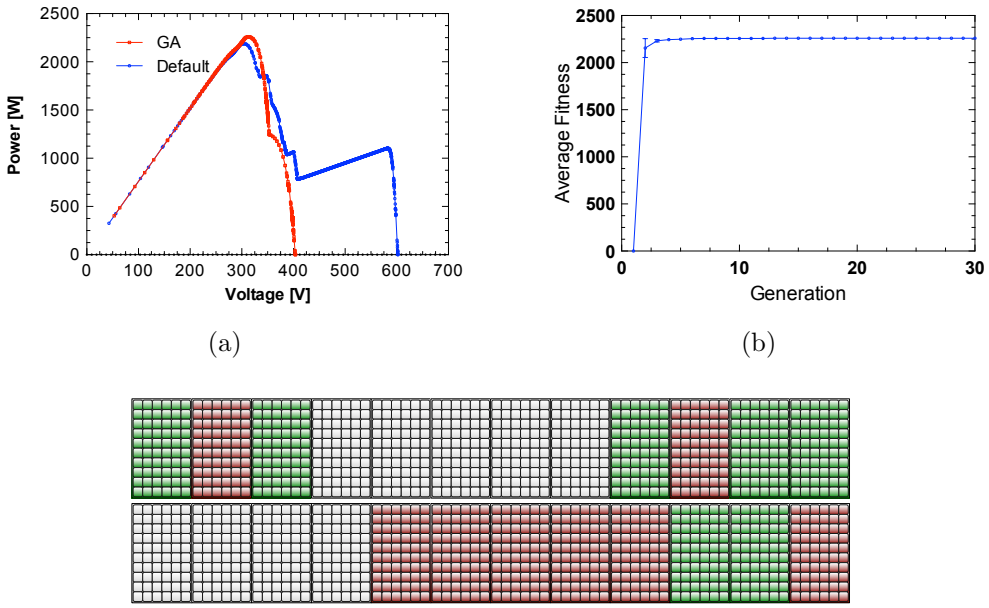

Figure 9: Pole shadow. Top pane (a): Voltage-Power characteristics of the PV field. Best solution obtained by the GA (blue line), default configuration (black line). Top pane (b): evolution of the best fitnesses averaged over 20 runs. Mean fitness (blue line) +/− standard deviation. Bottom pane (c): electrical configuration chosen by the GA.

The effect of partially shaded panels determines V-P characteristic of the field exhibiting many local MPPs (see Figure 10(b)). The global maximum power value is equal to 3007.69W @ V_{mpp} 418.54V, while the standard configuration shows a MPP equal to 2993.32W V_{mpp} @ 416.5V.

Only 20 generations are required in order to obtain the desired solution, as shown in the fitness evolution graph (Figure 10(c)). The same fitness evolution is always obtained, so standard deviation (red dotted) and average fitness (blue) lines overlap.

4.3.3. Gradual shadowing

Case 4. (see Fig. 4.1.3). As expected, the most shaded panels have been disconnected by the proposed GA (see Fig. 11(a)). The optimal electrical configuration is, again, obtained by disposing the equal radiated panels in the same string.

The default configuration is really inefficient when this kind of solar ra-

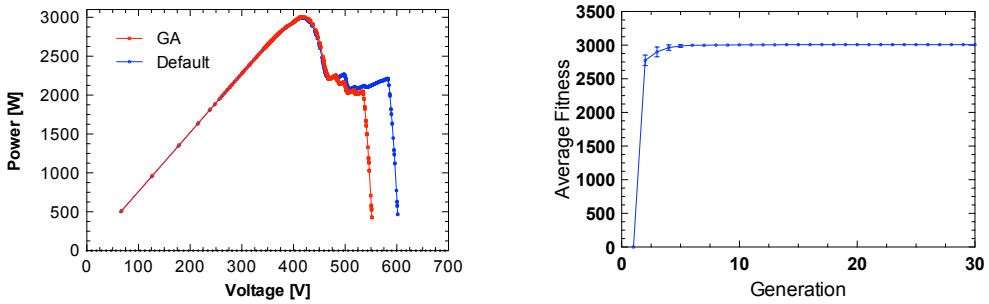

(a) (b)

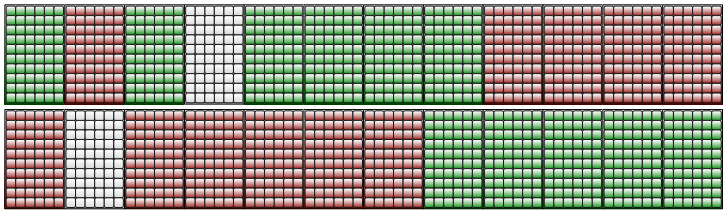

(c)

Figure 10: Cable shadow. Top pane (a): Voltage-Power characteristics of the PV field. Best solution obtained by the GA (blue line), default configuration (black line). Top pane (b): evolution of the best fitnesses averaged over 20 runs. Mean fitness (blue line) +/− standard deviation. Bottom pane (c): electrical configuration chosen by the GA.

diance scenario occurs. In fact, the V-P characteristic of the default configuration exhibits many different local MPPs and the maximum power that can be extracted is equal to 1510W @ V_{mpp} 431.5V. The V-P characteristic of the best solution, illustrated in Figure 11(b), exhibits some unimportant lower MPP close to the global one having a power value equal to 2199.98W @ V_{mpp} 461.87V. In comparison with the symmetrical gradual shadow, only an optimal solution has been found, so, in the fitness evolution plot (see Fig. 11(c)), the standard deviation is expected to be zero after the highest fitness has been reached. The best optimal configuration is obtained after only 20 generations.

4.3.4. Spot shadowing

Case 5. (see Fig. 7). Since there is not a precise geometrical solar irradiance pattern, in this case it is very difficult to predict which electrical configuration could be the optimal one. For this scenario, three different so-

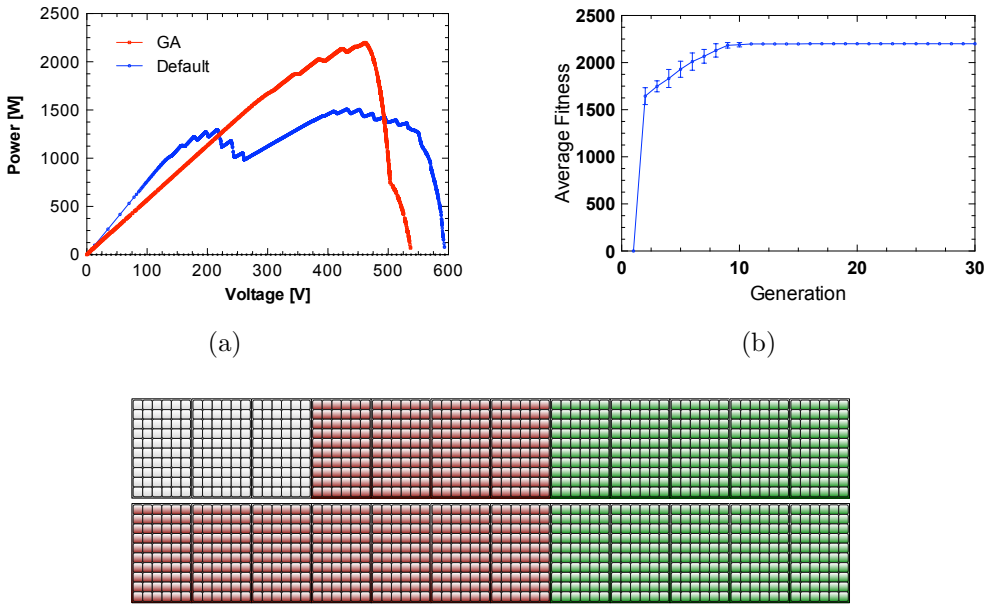

Figure 11: Asymmetrical gradual shadow. Top pane (a): Voltage-Power characteristics of the PV field. Best solution obtained by the GA (blue line), default configuration (black line). Top pane (b): evolution of the best fitnesses averaged over 20 runs. Mean fitness (blue line) +/− standard deviation. Bottom pane (c): electrical configuration chosen by the GA.

lutions have been found by the GA during the 20 runs. In all these solutions, no panels have been disconnected.

With reference to the default configuration, whose V-P characteristic exhibits a maximum power peak value equal to 2194.035W @ 497.545 V, the solutions chosen by GA improves the power generation at least by 7%.

In fact, for the first configuration (see Figure 12(a)), the maximum power is equal to 2362.02W @ Vmpp: 472.20V. The corresponding V_{mpp} voltage value is lower than those in the other two solutions and a higher mismatch has been verified in the correspondent voltage power characteristic (Fig. 13(a), green line). Instead, a different arrangement of the panels (see Figures 12(b) and 12(c)) increases both the voltage and the generated power (Fig. 13(a), blue and red lines). In Fig. 13(a), the difference between the global power peaks of the blue and red V-P characteristics, as well as that of their V_{mpp} values, is not significant. In fact, the MPPs values are respectively equal to

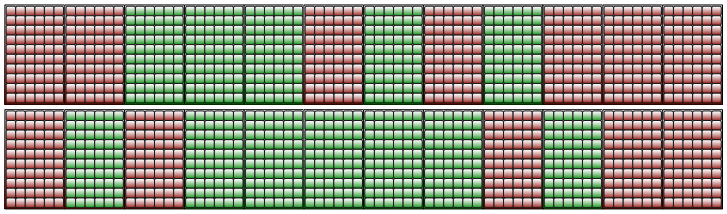

(a)

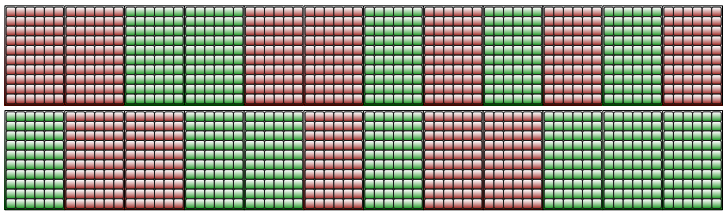

(b)

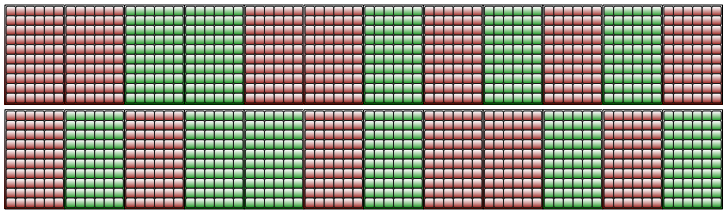

(c)

Figure 12: Spot shadowing. The three electrical configurations chosen by GA.

2365.44W @ V_{mpp} 506.28V and 2407.85W @ V_{mpp} 505.28V.

The trend of fitness evolution appears very abrupt, as shown in Figure 13(b), but, for this scenario, the number of generations required to achieve the best configurations is much greater than other case studies.

In fact, the average fitness (blue line) clearly increases during all the 200 generations. So, in this case, an higher number of generations (i.e. 150) is required to find the optimal solution.

5. Conclusions

In this paper an evolutionary based approach to the dynamical reconfiguration of photovoltaic fields is presented. The algorithm is designed by

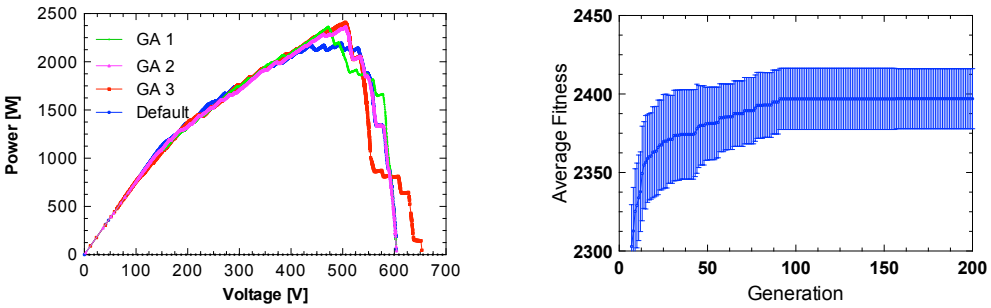

(a) (b)

Figure 13: Spot shadowing. Left Pane: Voltage-Power characteristics of the PV fieldSpot shadowing. Right Pane: evolution of the best fitnesses averaged over 20 runs. Mean fitness (blue line) +/- standard deviation.

having as a final target the implementation on an embedded system for on-field applications. The approach has been validated by means of a large number of simulated scenarios reproducing real cases. The genetic algorithm is robust and it is able to achieve the optimal solution in a small percentage of the number of generations run, this being a feature for its on-field use. The evaluation of the fitness function represents the main computational burden of the algorithm. This limitation is overcome by a suitable pre-processing of the panels characteristics by means of an algorithm that is able to extract their fingerprints, thus reducing very greatly the number of samples needed for describing the electrical behavior of each panel. This further step allows the final porting of the algorithm on an embedded device with a computation time not greater that 1 minute.

6. Acknowledgements

The authors acknowledge the support from FARB funds of the University of Salerno.

7. References

[1] Axitec solar panels - model ac-250m/156-60s.

[2] G. Adinolfi, N. Femia, G. Petrone, G. Spagnuolo, M. Vitelli, Design of dc-dc converters for dmppt pv applications based on the concept of

energetic efficiency, Journal of Solar Energy Engineering, Transactions of the ASME 132 (2) (2010) 0210051–02100510.

[3] C. W. Ahn, Advances in Evolutionary Algorithms: Theory, Design and Practice, vol. 18 of Studies in Computational Intelligence, Springer, 2006.

[4] T. Bäck, Evolutionary Algorithms in Theory and Practice: Evolution Strategies, Evolutionary Programming, Genetic Algorithms, Oxford University Press, Oxford, UK, 1996.

[5] J. Bishop, Computer simulation of the effects of electrical mismatches in photovoltaic cell interconnection circuits, Solar Cells 25 (1) (1988) 73–89.

[6] P. Carotenuto, P. Manganiello, G. Petrone, G. Spagnuolo, Online recording a pv module fingerprint, IEEE Journal of Photovoltaics PP (99) (2014) 1–10.

[7] P. L. Carotenuto, P. Manganiello, G. Petrone, G. Spagnuolo, About the criteria for triggering the reconfiguration of a photovoltaic array, in: Industrial Electronics (ISIE), 2014 IEEE 23rd International Symposium on, IEEE, 2014.

[8] K.-H. Chao, L.-Y. Chang, H.-C. Liu, Maximum power point tracking method based on modified particle swarm optimization for photovoltaic systems, International Journal of Photoenergy 2013.

[9] Y. Davidor, Epistasis variance: A viewpoint on ga-hardness, in: FOGA, 1990.

[10] N. Femia, G. Petrone, G. Spagnuolo, M.Vitelli, Power Electronics and Control Techniques for Maximum Energy Harvesting in Photovoltaic Systems, CRC Press, 2013.

[11] S. Forrest, M. Mitchell, Relative building-block fitness and the building block hypothesis, in: FOGA, 1992.

[12] D. E. Goldberg, Genetic Algorithms in Search, Optimization and Machine Learning, 1st ed., Addison-Wesley Longman Publishing Co., Inc., Boston, MA, USA, 1989.

[13] D. Gómez-Lorente, I. Triguero, C. Gil, A. Espín Estrella, Evolutionary algorithms for the design of grid-connected pv-systems, Expert Systems with Applications 39 (9) (2012) 8086–8094.

[14] J. H. Holland, Adaptation in Natural and Artificial Systems: An Introductory Analysis with Applications to Biology, Control and Artificial Intelligence, MIT Press, Cambridge, MA, USA, 1992.

[15] Kolarov, Landscape ruggedness in evolutionary algorithms, in: Proceedings of The IEEE Conference on Evolutionary Computation, IEEE World Congress on Computational Intelligence, 1997.

[16] A. Kornelakis, Multiobjective particle swarm optimization for the optimal design of photovoltaic grid-connected systems, Solar Energy 84 (12) (2010) 2022–2033.

[17] M. Mitchell, J. H. Holland, When will a genetic algorithm outperform hill climbing?, in: ICGA, 1993.

[18] M. Miyatake, F. Toriumi, N. Fujii, H. Ko, et al., Maximum power point tracking of multiple photovoltaic arrays: a pso approach, Aerospace and Electronic Systems, IEEE Transactions on 47 (1) (2011) 367–380.

[19] H. Obane, K. Okajima, T. Oozeki, T. Ishii, Pv system with reconnection to improve output under nonuniform illumination, IEEE Journal of Photovoltaics 2 (3) (2012) 341–347.

[20] C. Olalla, C. Deline, D. Maksimovic, Performance of mismatched pv systems with submodule integrated converters, IEEE Journal of Photovoltaics 4 (1) (2014) 396–404.

[21] M. Orozco-Gutierrez, J. Ramirez-Scarpetta, G. Spagnuolo, C. Ramos-Paja, A method for simulating large {PV} arrays that include reverse biased cells, Applied Energy 123 (0) (2014) 157–167.

[22] R. Ramaprabha, Selection of an optimum configuration of solar pv array under partial shaded condition using particle swarm optimization.

[23] K. Ro, S. Rahman, Two-loop controller for maximizing performance of a grid-connected photovoltaic-fuel cell hybrid power plant, Energy Conversion, IEEE transactions on 13 (3) (1998) 276–281.

[24] E. Romero-Cadaval, G. Spagnuolo, L. Garcia Franquelo, C. Ramos-Paja, T. Suntio, W. Xiao, Grid-connected photovoltaic generation plants: components and operation, IEEE Industrial Electronics Magazine 7 (3) (2013) 6–20.

[25] F. Rothlauf, Representations for evolutionary algorithms, in: GECCO (Companion), 2014.

[26] M. Shamseldein, M. Kazerani, M. Salama, Reconfigurable photovoltaic structure, -US Patent App. 13/354,876 (May 10 2012).
URL http://www.google.com/patents/US20120111391

[27] D. J. Sheskin, Handbook of Parametric and Nonparametric Statistical Procedures, 4th ed., Chapman & Hall/CRC, 2007.

[28] H. Taheri, Z. Salam, K. Ishaque, et al., A novel maximum power point tracking control of photovoltaic system under partial and rapidly fluctuating shadow conditions using differential evolution, in: Industrial Electronics & Applications (ISIEA), 2010 IEEE Symposium on, IEEE, 2010.

[29] M. Veerachary, T. Senjyu, K. Uezato, Neural-network-based maximum-power-point tracking of coupled-inductor interleaved-boost-converter-supplied pv system using fuzzy controller, Industrial Electronics, IEEE Transactions on 50 (4) (2003) 749–758.

[30] L. Villa, D. Picault, B. Raison, S. Bacha, A. Labonne, Maximizing the power output of partially shaded photovoltaic plants through optimization of the interconnections among its modules, IEEE Journal of Photovoltaics 2 (2) (2012) 154–163.

[31] WebSite:.
URL http://www.solaredge.com/

[32] WebSite:.
URL http://enphase.com/

[33] WebSite:.
URL http://www.tigoenergy.com/

[34] WebSite: (2013).
URL http://www.bitronenergy.com/